Supplemental Data

Attenuated TGFβ Signaling Promotes Nuclear Factor-κB Activation in Head and Neck Cancer

Jonah Cohen, Zhong Chen, Shi-Long Lu, Xin Ping Yang, Pattatheyil Arun, Reza Ehsanian, Matt Brown, Hai Lu, Bin Yan, Oumou Diallo, Xiao-Jing Wang, and Carter Van Waes

Supplemental Experimental Procedures

Cell Proliferation Assay

HeKa and HNSCC cells were initially plated in quadruplicate onto a 96-well plate at 5 x 10^3 cells per well in 100 µl of complete MEM. The next day, cells were exposed to different concentrations of recombinant active TGFβ1 and and cell proliferation was analyzed at 0, 1, 3 and 5 days using a 3-(4,5-dimethylthiazol-2-yl)-2,5-diphenyltetrazolium bromide (MTT) Cell Proliferation kit (Roche Diagnostics) as described by others (1). The optical density was measured by a microplate reader at a wavelength of 570 nm.

Real-time QRT-PCR Conditions

Amplification conditions for all QRT-PCR reactions were: activation of enzymes for 2 min at 50°C and 10 min at 95°C, followed by 40 cycles at 15 s at 95°C and 1 min at 60°C.

Thermal cycling and fluorescence detection were done using an ABI Prism 7700 Sequence Detection System (Applied Biosystems).

Luciferase Reporter Assays

Transfection and NF-κB reporter assays were done as described previously (2). Briefly, UM-SCC cells were seeded in 24-well plates as triplicates and transiently transfected with the indicated expression construct, reported plasmid, and β-galactosidase control vector, and lysates were analyzed at the indicated time using the Dual-Light Combined Reporter Gene Assay System (Tropix). For TGFβ-induced reporter activity, the p3TP-Luc reporter plasmid (3) was kindly provided by the laboratory of Dr. Stuart Yuspa (National Institutes of Health, Bethesda, MD). The p3TP-Luc construct serves as a specific readout for TGFβ-mediated signaling (4). The IκB-luciferase nontranscriptional reporter was kindly provided by the laboratory of Dr. Louis M. Staudt. The IκBα-*Photinus* luciferase fusion protein serves as an indicator of IKK activity (5).

Immunohistochemistry and Immunofluorescence

Immunohistochemistry (IHC) for TβRII, p-Smad2, and TP53 was performed using standard methods (6). A semiquantitative scoring of IHC staining was performed from a representative high power field from 3 tissue array spots each for 20 tumor specimens and 2 spots each for normal oral mucosa specimens by three independent investigators using predetermined standards of negative (-), weak (Low), and strongly positive (+), staining intensity for representative high-power fields. These scores were collated and assigned to the proteins TβRII, p-Smad2 and TP53 for each tumor specimen. As there was no inconsistency in patterns between the triplicate or duplicate samples, or inter-

observer variability except for 1/20 specimens for the semi-quantitative method used, no variance or statistical analysis of the measures themselves were performed.

Regarding murine samples, H&E and immunohistochemical staining for TβRII and p-Smad2 were performed as previously described (7, 8). Double-stain immunofluorescence was performed as described previously (9). Briefly, paraffin-embedded sections were deparaffinized, and antigen retrieval was performed by microwaving slides in 10 mmol/L sodium citrate solution for 10 minutes. Each section was incubated with a primary antibody, phosphorylated-p65 (Cell Signaling) or p50 (Santa Cruz) diluted in PBS containing 12% bovine serum albumin, together with a guinea pig antiserum against mouse keratin 14 (K14, Fitzgerald). The section were then washed with PBS and incubated with fluorescence dye-conjugated secondary antibodies, an Alexa Fluor 488-conjugated (green) secondary antibody against the species of the primary antibody (Molecular Probes), and Alexa Fluor 594-conjugated (red) anti-guinea pig secondary antibodies (Molecular Probes) for 30 minutes at room temperature. Sections were visualized under a Nikon Eclipse E600W fluorescence microscope.

Western Blot

Proteins were separated by electrophoresis on 4-12% gradient gels (Invitrogen), transferred to nitrocellulose membranes and subjected to immunoblotting. Membranes were blocked in 5% non-fat milk in Tris Buffered Saline containing 0.1% Tween-20. Primary antibodies were used at the indicated concentrations, and HRP-coupled secondary antibodies were generally used at 1:2000. Immunoblots were developed

using Super Signal West Pico substrate (Pierce). Quantitative densitometry was performed using PDI Quantity One software (Bio-Rad) as previously reported (10).

Statistical Analysis

Statistical differences between two groups of data were analyzed using the Student's *t*-test. The data are presented as mean ± standard deviation (SD) with the exception of the data in Figure 7, which are presented as mean ± standard error (SE)

References

1. Carmichael J, DeGraff WG, Gazdar AF, Minna JD, Mitchell JB. Evaluation of a tetrazolium-based semiautomated colorimetric assay: assessment of chemosensitivity testing. Cancer Res 1987;47:936-42.
2. Bancroft CC, Chen Z, Yeh J, et al. Effects of pharmacologic antagonists of epidermal growth factor receptor, PI3K and MEK signal kinases on NF-kappaB and AP-1 activation and IL-8 and VEGF expression in human head and neck squamous cell carcinoma lines. Int J Cancer 2002;99:538-48.
3. Wrana JL, Attisano L, Carcamo J, et al. TGF beta signals through a heteromeric protein kinase receptor complex. Cell 1992;71:1003-14.
4. Dennler S, Itoh S, Vivien D, ten Dijke P, Huet S, Gauthier JM. Direct binding of Smad3 and Smad4 to critical TGF beta-inducible elements in the promoter of human plasminogen activator inhibitor-type 1 gene. EMBO J 1998;17:3091-100.
5. Lam LT, Davis RE, Pierce J, et al. Small molecule inhibitors of IkappaB kinase are selectively toxic for subgroups of diffuse large B-cell lymphoma defined by gene expression profiling. Clin Cancer Res 2005;11:28-40.
6. Van Waes C, Chang AA, Lebowitz PF, et al. Inhibition of nuclear factor-kappaB and target genes during combined therapy with proteasome inhibitor bortezomib and reirradiation in patients with recurrent head-and-neck squamous cell carcinoma. Int J Radiat Oncol Biol Phys 2005;63:1400-12.
7. Lu SL, Herrington H, Reh D, et al. Loss of transforming growth factor-beta type II receptor promotes metastatic head-and-neck squamous cell carcinoma. Genes Dev 2006;20:1331-42.
8. Lu SL, Reh D, Li AG, et al. Overexpression of transforming growth factor beta1 in head and neck epithelia results in inflammation, angiogenesis, and epithelial hyperproliferation. Cancer Res 2004;64:4405-10.
9. Li AG, Wang D, Feng XH, Wang XJ. Latent TGFbeta1 overexpression in keratinocytes results in a severe psoriasis-like skin disorder. EMBO J 2004;23:1770-81.
10. Yamin TT, Ayala JM, Miller DK. Activation of the native 45-kDa precursor form of interleukin-1-converting enzyme. J Biol Chem 1996;271:13273-82.

Supplemental Table 1

Tumor and Outcome Characteristics of Patients Providing Human HNSCC Cell Lines

Cell line	Age	Sex	Stage	TNM	Primary site	Specimen site	Survival
UM-SCC 1	72	M	I	T1N0M0	FOM	Local recur	15
UM-SCC 6	37	M	II	T2N0M0	Tongue	Pri bx	LTF
UM-SCC 9	72	F	II	T2N0M0	Tonsil/BOT	Local recur	15
UM-SCC 11A	65	M	V	T2N2aM0	Hypopharynx	Pri bx	14
UM-SCC 11B						Pri resect	
UM-SCC 22A	59	F	III	T2N1M0	Hypopharynx	Pri bx	10
UM-SCC 22B						LN met	
UM-SCC 38	60	M	IV	T2N2aM0	Tonsil/BOT	Pri	11
UM-SCC 46	57	F	III	None given	Supraglottic larynx	Local recur	6

The clinical information was kindly provided by Drs. Thomas E. Carey and Carol R. Bradford, and some information was presented previously in the literature. 'Age' represents age at diagnosis in years. 'Primary site' refers to the origin of the primary tumor. 'Specimen site' refers to origin of tissue used to establish cultures. 'Survival' represents time in months from diagnosis to last follow up. BOT, base of tongue; bx, biopsy; F, female; FOM, floor of mouth; LN, lymph node; LTF, lost to follow-up; M, male; met, metastasis; Pri, primary tumor site; recur, recurrence; resect, surgical resection specimen; HNSCC, head and neck squamous cell carcinoma; TNM, tumor-node-metastasis (staging system); UM-SCC, University of Michigan series head and neck squamous cell carcinoma.

Supplemental Table 2

Sequencing Analysis of *TP53* in UM-SCC Cell Lines

Cell line	TP53 mutation	Type of mutation
UM-SCC 1	wt	N/A
UM-SCC 6	wt	N/A
UM-SCC 9	wt	N/A
UM-SCC 11A	wt	N/A
UM-SCC 11B	Exon 7, 242 TGC → TCC	Missense by transversion (Cysteine → Serine)
UM-SCC 22A	Exon 6, 220 TAT → TGT	Missense by transition (Tyrosine → Cysteine)
UM-SCC 22B	Exon 6, 220 TAT → TGT	Missense by transition (Tyrosine → Cysteine)
UM-SCC 38	Exon 5, 132 AAG → AAT	Missense by transversion (Lysine → Asparagine)
UM-SCC 46	Exon 8, 278 CCT → GCT	Missense by transversion (Proline → Alanine)

The *TP53* genotype of nine University of Michigan series head and neck squamous cell carcinoma (UM-SCC) cell lines was analyzed by two-directional sequencing exons four to nine.

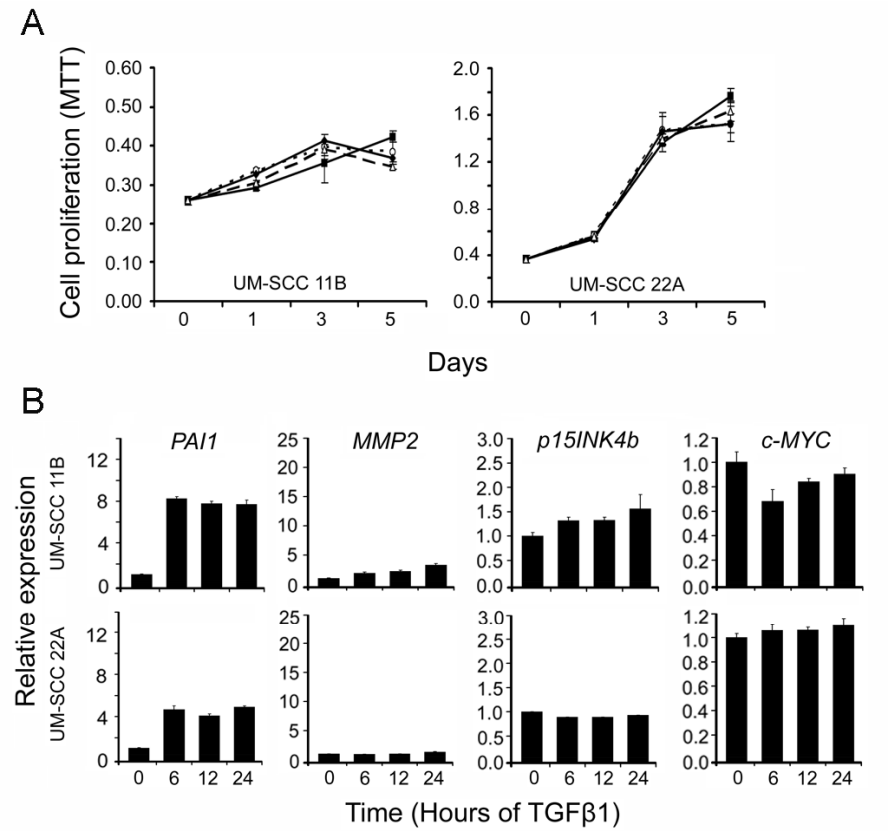

Supplementary Figure 1. Attenuated TGFβ-Induced Growth Inhibition and Target Gene Expression in HNSCC Cells. **(A)** Functional attenuation of TGFβ-mediated growth arrest in UMSCC lines. Cell proliferation was measured in 5-day MTT assay in HeKa cells and UM-SCC lines of differing TP53 status. Cells were treated with 1, 10 or 20 ng/ml of rTGFβ1. Cell growth rates were analyzed in quadruplicate, mean±SD, *p<0.05. **(B)** Attenuated TGFβ-induced activation of *PAI1*, *MMP2*, and *p15INK4b* and suppression of *c-MYC* in UM-SCC. UM-SCC lines and HeKa cells were stimulated with 10 ng/ml for indicated time-points, and total RNA was isolated and assayed for TGFβ target gene mRNA levels by QRT-PCR. Expression of individual genes at 0 hr were set to the value of 1 arbitrary unit. Means±SD between triplicate samples are shown.

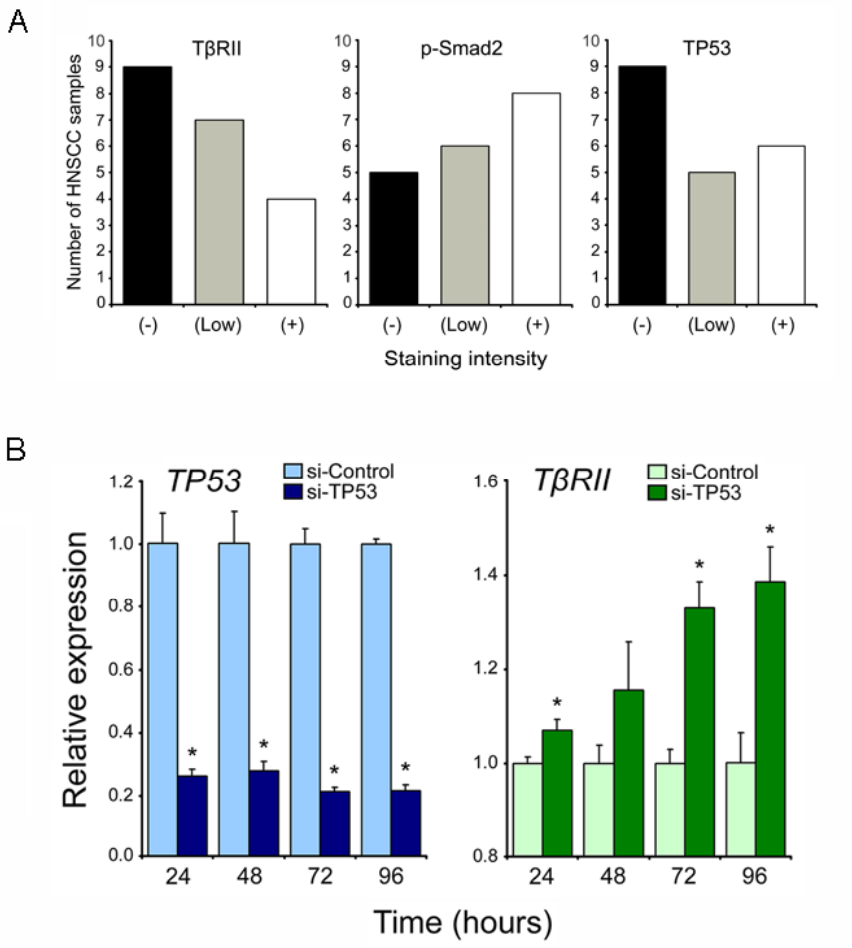

Supplementary Figure 2. Diminished TβRII Expression and Signaling, Mutant TP53 Accumulation and NF-κB Target Gene Activation in a subset of HNSCC. (A) Semi-quantitative scoring and classification of TβRII, p-Smad2 and TP53 protein staining of 20 tumors was performed as described in supplemental methods: (–), negative; (low), reduced; (+), strong staining. **(B)** TP53 siRNA knockdown enhances TβRII expression in mt*TP53* UM-SCC-22A. Quantitation of mtTP53 inhibition and target genes was assessed using QRT-PCR at the indicated time points. The expression level in each control siRNA-treated sample is designated as 1.0. Means±SD between triplicate samples, *p<0.05 are shown.

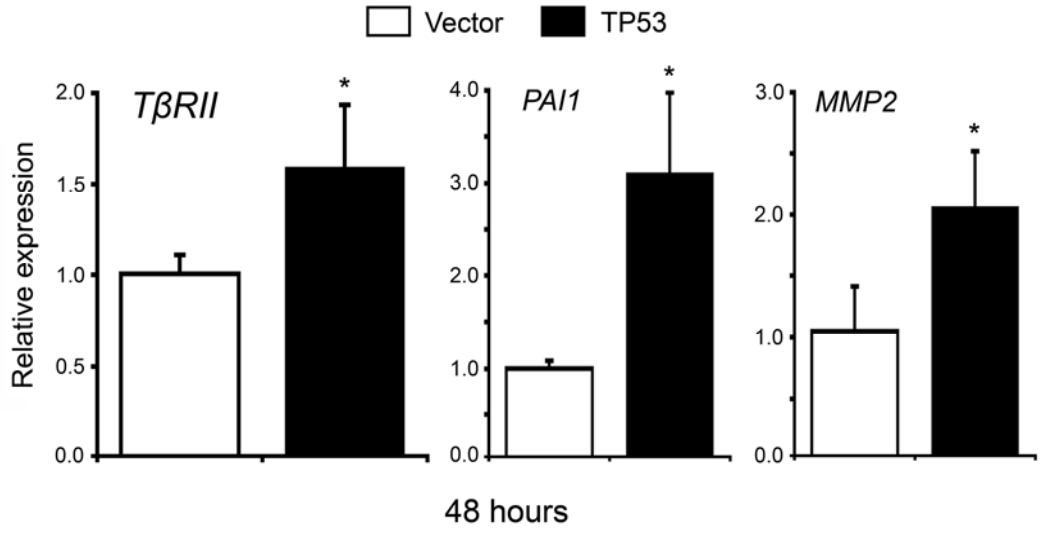

Supplemental Figure 3

Wild-type *TP53* Transfection into TP53-Deficient HNSCC Cells Restores *TβRII* Expression and TGFβ Signaling. UM-SCC 11A demonstrates enhanced *TβRII* expression measured by quantitative RT-PCR at 48 hr following transfection with a wild-type human *TP53* expression plasmid compared to control vector. Further, restored expression of *TβRII* augments TGFβ signaling as evidenced by strong induction of downstream genes, *PAI1* and *MMP2*.

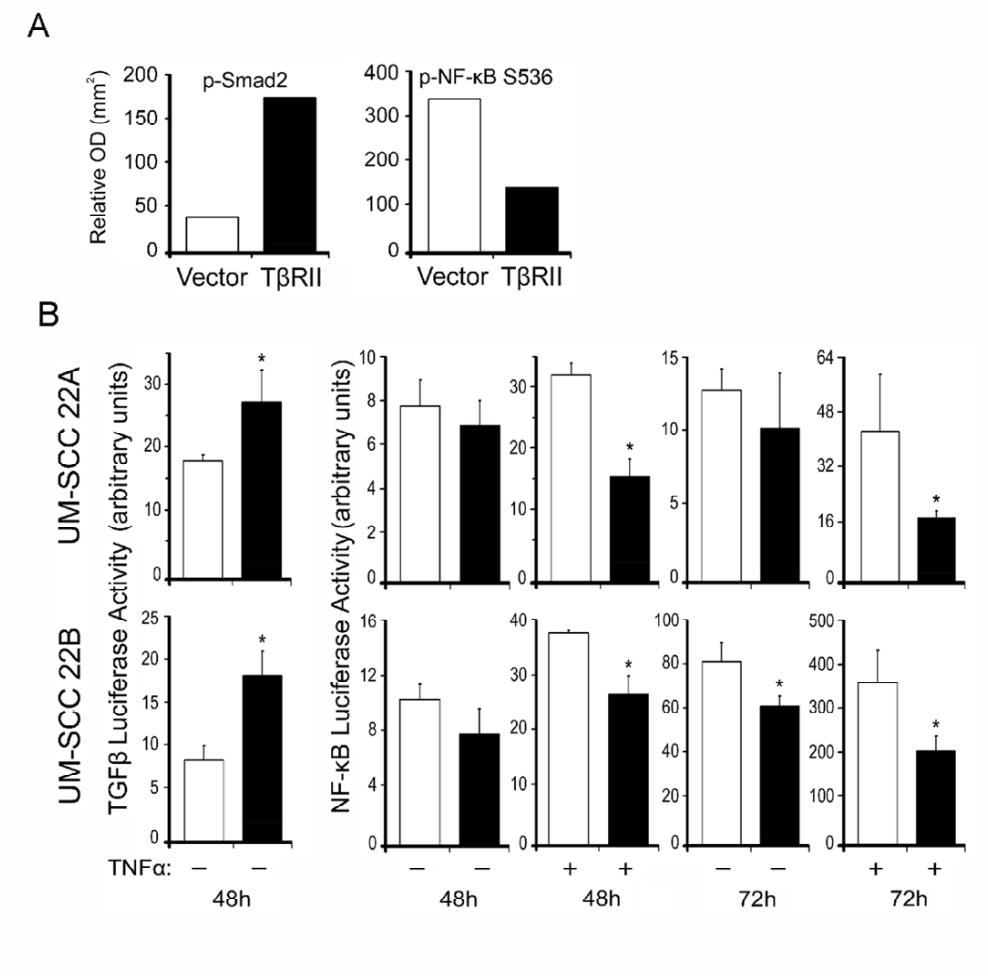

Supplementary Figure 4. TβRII induces TGFβ and attenuates NF-κB reporter gene transactivation in UM-SCC. HNSCC lines were co-transfected with the respective reporter plasmid plus a *TβRII* expression or control vector, and cultured ±TNFα (10 ng/ml) for 12 hr prior to the indicated time-points. **(A)** Densitometric quantification of western analysis of nuclear extracts from UM-SCC-46 showing re-expression of TβRII for 48 hrs restores TGFβ phospho-Smad2 signaling, and suppresses IKK-dependent serine-536 after TNFα (10 ng/ml). Densitometric quantification of p-Smad2 and p-NF-κB S536protein is shown. **(B)** TβRII induces TGFβ and attenuates NF-κB reporter gene transactivation in UM-SCC. HNSCC lines were co-transfected with the respective

reporter plasmid plus a *TβRII* expression or control vector, and cultured ±TNFα (10 ng/ml) for 12 hr prior to the indicated time-points. All luciferase values are normalized to β-galactosidase. Bar graphs indicate mean±SD of triplicate samples, *$p<0.05$.

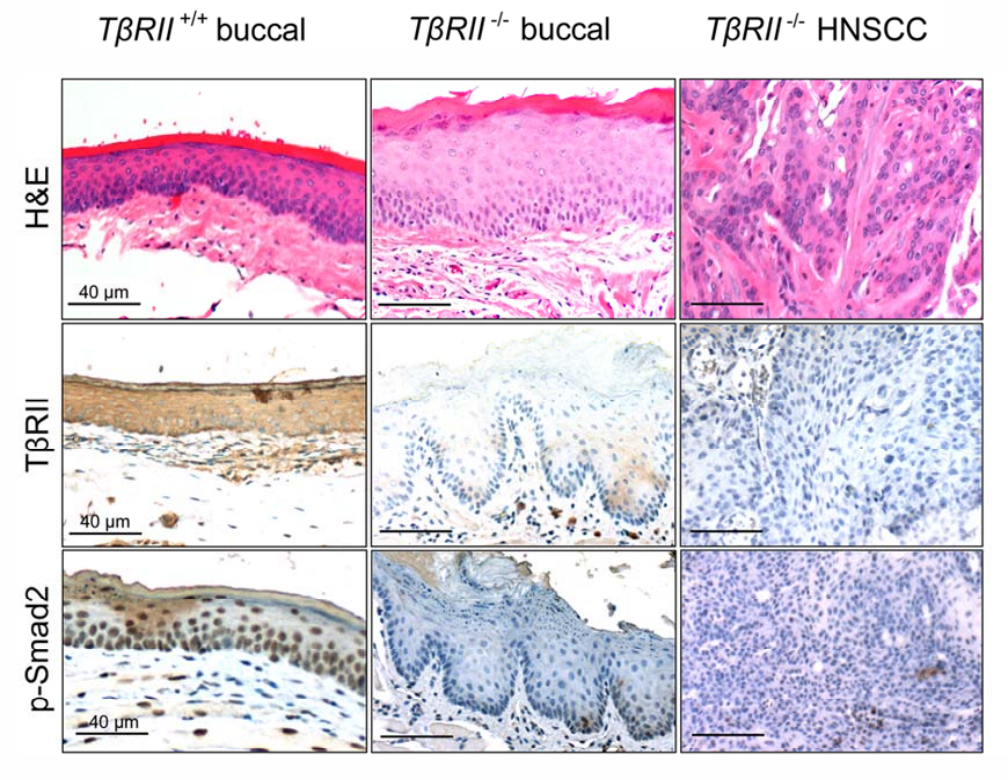

Supplementary Figure 6. Abrogation of TGFβ Signaling Promotes NF-κB Activation and Proinflammatory Target Gene Expression in HNSCCs of *TβRII*$^{-/-}$ Mice. H&E, TβRII, p-Smad2 IHC staining of buccal squamous mucosa from TβRII$^{+/+}$, TβRII$^{-/-}$ and HNSCC from TβRII$^{-/-}$ mice. Buccal tissues representative of 5 *TβRII*$^{+/+}$ and *TβRII*$^{-/-}$ mice at 3 months and HNSCC from 5 *TβRII*$^{-/-}$ mice at 6 months following DMBA initiation are shown.